Hierarchical path planning for multi-size agents in heterogenous environments

Daniel Harabor and **Adi Botea**
National ICT Australia and The Australian National University
{ daniel.harabor | adi.botea } at nicta.com.au

Abstract

In this paper we present new techniques for the automated construction of state space representations of complex multi-terrain grid maps with minimal information loss. Our approach involves the use of graph annotations to record the amount of maximal traversable space at each location on a map. We couple this with a cluster-based hierarchical abstraction technique to build highly compact yet complete representations of the original problem. We further outline the design of a new planner, Annotated Hierarchical A* (AHA*), and demonstrate how a single abstract graph can be used to plan for many different agents, including different sizes and terrain traversal capabilities. Our experimental analysis shows that AHA* is able to generate near-optimal solutions to a wide range of problems while maintaining an exponential reduction in comparative effort over low-level search. Meanwhile, our abstraction technique is able to generate approximate representations of large problem-spaces with complex topographies using just a fraction of the storage space required by the original grid map.

Introduction

Single-agent path planning is a well known and extensively studied problem in computer science. It has many applications such as logistics, robotics, and more recently, computer games. Despite the large amount of progress that has been made in this area, to date, very little work has focused specifically on addressing planning for diverse-size agents in heterogenous terrain environments.

The problem is interesting because such diversity introduces much additional complexity when solving route-finding problems. Modern real-time strategy or role-playing games for example often feature a wide array of units of differing shapes and abilities that must contend with navigating across environments with complex topographical features – many terrains, different elevations etc. Thus, a route which might be valid for an infantry-solider may not be valid for a heavily armoured tank. Likewise, a car and an off-road vehicle may be similar in size and shape but the paths preferred by each one could differ greatly.

Unfortunately, the majority of current path planners, including recent hierarchical planners ((Botea, Müller, and Schaeffer 2004), (Sturtevant and Buro 2005), (Demyen and Buro 2006), (Geraerts and Overmars 2007)), only perform well under certain ideal conditions. They assume, for example, that all agents are equally capable of reaching most areas on a given map and any terrain which is not traversable by one agent is not traversable by any. Further assumptions are often made about the size of each respective agent; a path computed for one is equally valid for any other because all agents are typically of uniform size. Such assumptions limit the applicability of these techniques to solving a very narrow set of problems: homogenous agents in a homogenous environment.

We address the opposite case and show how efficient solutions can be calculated in situations where both the agent's size and terrain traversal capability are variable. Our method extends recent work emerging from the areas of robotics and computer games which has shown the effectiveness of using clearance annotations to measure obstacle distance at key locations in the environment and using this information to help agents plan better paths.

We contribute in several ways: first, we introduce AHA*, a new clearance-based hierarchical path planner; second, we show how to leverage clearance in order to produce compact yet information rich search abstractions; third, we provide a detailed empirical analysis of our new technique on a wide range of problems involving multi-size agents in heterogenous multi-terrain environments.

The rest of this paper is organised as such: first, we cover existing work in the area of hierarchical path planning and multi-size agent search. We then define the problem and describe our map annotation approach before showing how to adapt A* to plan for a range of agents of different sizes and capabilities. We go on to detail a new map abstraction technique that leverages map annotations and characterise the worst-case performance. In the final sections we introduce our hierarchical planner, AHA*, and provide a detailed analysis of its performance before concluding.

Related Work

A very effective method for the efficient computation of path planning solutions is to make the original problem more tractable by creating and searching within a smaller approximate abstract space. Abstraction factors a search problem into many smaller problems and thus allows agents to reason about pathfinding strategies in terms of macro operations. This is known as hierarchical path planning.

Two recent hierarchial path planners relevant to our work are described in (Botea, Müller, and Schaeffer 2004) and (Sturtevant and Buro 2005). The first of these, HPA*, builds an abstract search graph by dividing the environment into square clusters connected by entrances. Planning involves inserting the low-level start and goal nodes into the abstract graph and finding the shortest path between them.
The second algorithm, PRA*, builds a multi-level search-space by abstracting cliques of nodes; the result is to narrow the search space in the original problem to a "window" of nodes along the optimal shortest-path. Both HPA* and PRA* are focused on solving planning problems for homogenous agents in homogenous-terrain environments and hence are not complete when either of these variables change. Our technique is similar to HPA* but we extend that work to solve a wider range of problems.

In robotics, force potentials help autonomous robots find collision-free paths through an environment. The basic intution is that a robot is attracted to the far-away goal and repulsed away from obstacles as it nears them. A well known method for potential-based path planning is the Brushfire algorithm (Latombe 1991), which proceeds by annotating each tile in a grid-map with the distance to the nearest obstacle. This embedded information allows the robot to calculate repulsive potentials and makes it possible to plan using a gradient descent strategy. Brushfire is similar to AHA* in that the annotations it produces allow an agent to know something about its proximity to a nearby obstacle. AHA* differs by explicitly calculating the maximal size of traversable space at each location on the map. Furthermore, unlike Brushfire, AHA* does not suffer from incompleteness which can occur when repulsive forces cancel each other out and lead the robot into a local minimum.

The Corridor Map Method (CMM) (Geraerts and Overmars 2007) is a recently introduced path planner able to answer queries for multi-size agents by using a *probabilistic roadmap* to represent map connectivity. The roadmap (or backbone path) is comprised of nodes which are annotated with clearance information that indicates the radius of a maximally sized bounding sphere before an obstacle is encountered. Nodes are placed on the roadmap by creating Voronoi regions to split the map and identify locations that maximise local distance from fixed obstacles.

Like CMM, AHA* calculates the amount of traversable space at a given location but our approach is adapted to grid environments, which are simpler to create than roadmaps and more commonly found in a range of applications. Another key difference is that we allow fine-grain control over the size of the abstract graph; CMM abstractions have a fixed size. Finally, we deal with multi-terrain cases making our method more information rich.

Representing an environment using navigation-meshes is increasingly popular in the literature. Two recent planners in this category are Triangulation A* and Triangulation Reduction A* (Demyen and Buro 2006). TA* makes use of a technique known as Delaunay triangulation to build a polygonal representation of the environment. This results in an undirected graph connected by constrained and unconstrained edges; the former being traversable and the latter not. TRA* is an extension of this approach that abstracts the triangle mesh into a structure resembling a roadmap. Like our method, both TA* and TRA* are able to answer path queries for multi-size agents. The abstraction approaches used by TA* and TRA* however are very distinctly different from our work. Where we use a simple division of the environment into square clusters, their approach aims to maximise triangle size. We also handle additional terrain requirements while both TA* and TRA* assume a homogenous environment.

Problem Definition

A *gridmap* is a structure composed of square cells, of unit size, each of which represent a unique area in the environment. Each grid cell is an *octile*, connected to k neighbours, where $0 \leq k \leq 8$.

Each octile, t, is associated with a particular terrain type, $terrain(t) \in T$ where T is the set of all possible terrains and there are $r = |T| : r \geq 1$ possible terrains. Each octile is either blocked or traversable. Blocked octiles are called *hard obstacles*, since no agent can occupy them.

Each gridmap is representable as a graph, $G = (V, E)$ where each traversable tile generates one node $v \in V$ and each cell adjacency is represented by an edge $e \in E$.

An *agent* is any entity attempting to move across a grid environment. Every agent is square in shape and has a size $s \geq 1 : s \in S$ where S is the set of finite sizes agents traversing across the gridmap may take. While stationary or moving, each agent occupies s^2 octiles which together correspond to its current location.

Agents can move in any of the four cardinal directions. Diagonal moves are allowed only if there exists an equivalent two-step move using the cardinal directions.

Every agent has a terrain traversal *capability*, $c \in C$, where c comprises a non-empty subset of terrains. An agent can never occupy a tile whose terrain type is not included in its capability.

A *soft obstacle* is a tile which is not traversable by a specific agent because it lacks the correct capability or its size is larger than the associated clearance value of the tile, as defined below.

A *clearance value* is an obstacle-distance metric associated with a particular tile in the grid environment. Each clearance value measures the maximal size of an agent at a given location without intersecting any obstacle in the environment. A tile can have several clearance values associated with it, one for each capability.

A *problem instance* is defined as a pair of locations, a start and goal, associated with an agent. A problem is valid if at least one path exists between the locations comprising only tiles traversable by the agent.

Computing Clearance Value Annotations

On a grid map, a clearance value is perhaps best explained as representing the length or width of a square that begins at some octile being evaluated and is expanded symmetrically to the right and down until it intersects an obstacle. To make our ideas more concrete we will use as a running example

a simple environment featuring two terrain types: Ground (represented as white tiles) and Trees (represented as grey tiles). To distinguish traversable tiles from non-traversable tiles we will colour hard obstacles black. The set of capabilities, C, required to traverse such a map is thus defined as $C = \{\{Ground\}, \{Trees\}, \{Ground \vee Trees\}\}$. We will work with agents of two sizes traversing across this environment and thus let $S = \{1, 2\}$.

Figure 1 (a) to (d) illustrates how clearance can be computed with an iterative procedure in an environment as described above. In Figure 1(a) the clearance square for the highlighted traversable target tile is initialised to 1. Subsequent iterations (Figures 1(b)-(c)) extend the square and increment the clearance. The process continues until the square contains an obstacle (Figure 1(d)) or extends beyond a map boundary at which point we terminate and do not increment clearance any further.

In Figure 1(e) we show the resultant clearance values for the single-terrain $\{Ground\}$ capability on a toy map example (note that we omit zero-value clearances). Similarly, Figure 1(f) and Figure 1(g) show the clearance values associated with the $\{Trees\}$ and $\{Ground \vee Trees\}$ capabilities respectively.

Figure 1: *(a)-(d) Computing clearance. (e)-(g) Clearance values for different capabilities.*

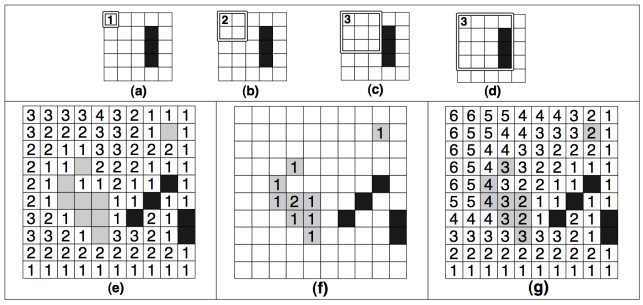

Once a clearance value is derived we store it in memory and repeat the entire procedure for each capability $c \in C$. The algorithm terminates when all octiles $t \in gridmap$ have been considered. The worst-case space complexity associated with computing clearance values in this fashion is thus characterised by:

Lemma 1. *Let CV be the set of all clearance values required to annotate an octile gridmap with r terrains. Further, let $G = (V, E)$ be a graph representing the gridmap where $V_{HO} \in V$ is the set of hard obstacles. Then,*

$$|CV| = (|V| - |V_{HO}|) \times 2^{r-1}$$

Proof. For a node to be traversable for some capability, the capability must include the node's terrain type. There are 2^r capabilities but each terrain type is included in only 2^{r-1} of these. There are $|V|$ nodes in total to represent the environment, and we avoid storing any clearance values for all nodes in V_{HO}. □

The result from Lemma 1 is an upper bound; if no agent has a given capability c there is no need to store the corresponding clearances. Despite this observation, the associated exponential growth function suggests that it is impractical to store every clearance value as there are $\Theta(2^r)$ per node. Fortunately, clearance values can be computed on-demand with little effort. In particular, calculating clearance for any agent a of size $s \in S$ only requires building a clearance square of maximum area s^2 octiles. We present such an approach in Algorithm 1.

Algorithm 1 Calculate Octile Clearance Value

Require: $t \in gridmap$ and $c \in C$ and $s \in S$
  $square \leftarrow t$
  $cv \leftarrow 0$
  while $traversable(square, c) \wedge area(square) \leq s^2$ **do**
    $cv \leftarrow cv + 1$
    $square \leftarrow expand(square)$
  return cv

The key advantage of calculating clearance is that we are able to plan for both large and small agents using a fixed size grid. We achieve this by mapping our extended problem into a classical problem with only two types of tiles (traversable and blocked) and reducing the problem to the case of a small-size agent that occupies the upper-left corner of the area required by the original, large-size agent.

Theorem 2. *Given an annotated grid map, any search problem involving an agent of arbitrary size and capability can be reduced into a small-agent search problem, where the size of the small agent is one tile and the capability of the agent is one terrain.*

Proof. A tile t is only traversable by an agent a if t has a clearance value cv_t associated with the agent's capability c_a which is at least as large as the size of the agent, s_a.

$$t(c_a) = cv_t \geq s_a : terrain(t) \subseteq c_a \in C, s_a \in S \qquad (1)$$

If equation 1 holds, it must be the case that the terrain type of every tile in the clearance square used to compute cv_t is included in c_a and hence traversable for the agent. Thus, the agent is able to navigate across a map by only considering the traversal requirements of a single node. Since each tile being evaluated is either traversable or not this is equivalent to solving a single-terrain problem. □

This is a useful result because it indicates that we can apply abstraction techniques from classical path planning to answer much more complex queries involving a wide range of terrain type and agent-size variables.

Annotated A*

Low-level planning for diverse sets of agents using clearance values is a straightforward application of the ideas thus far. We use a variation on the A* algorithm (Hart, Nilsson, and Raphael 1968) to compute an optimal shortest path between a start and goal node. Our approach differs from standard A* by requiring two additional parameters for each query: the agent's size and capability. This allows us to map any query into an instance of small-agent search as shown earlier by using the parameters to evaluate nodes before they are added

to A*'s open list. We term the resultant algorithm Annotated A* (AA* for short).

Cluster-based Map Abstraction

AA* is sufficient for low-level planning on the original gridmap but inefficient for large problem sizes; we would prefer to express a more general strategy using macro-operators. Our result from theorem 2 is key to the spatial abstraction described in this section.

We extend the process in (Botea, Müller, and Schaeffer 2004) which involves dividing a grid map into fixed-size square sections called *clusters*. Figure 2(a) shows the result of this decomposition approach; we use clusters of size 5 to split our toy map into 4 adjacent sections.

In the original work *entrances* are defined as obstacle-free transition areas of maximal size that exist along the border between two adjacent clusters. Each entrance has one or two transition points (depending on its size) which are represented in the abstract graph by a pair of nodes connected with an undirected *inter-edge* of weight 1.0. We use a similar approach but require as a parameter C, the set of all capabilities, and thus attempt to identify entrances for each $c \in C$.

Figure 2: *Building clusters and identifying entrances*

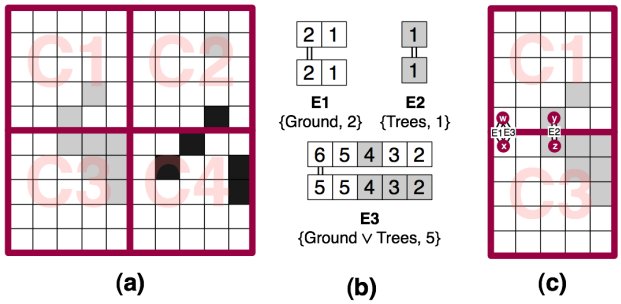

We start at the first pair of traversable tiles along the adjacent border area and extend each entrance until one of three termination conditions occurs: the end of the border area is reached, an obstacle is detected or the clearance value of nodes along the border area in either cluster begins to increase. The last condition is important to preserve representational completeness for large agents in cases where a cluster is partially divided by an obstacle (such as a wall) near the border. By leveraging clearance we are able to reason about the presence of such obstacles and build a new entrance each time we detect the amount of traversable space inside either cluster is increasing.

Once an entrance is found, we choose as the transition point the first pair of adjacent nodes in each cluster which maximise clearance for c. This latter metric, cv_{inter} is computed by taking the minimum clearance among each pair of adjacent nodes in the entrance area and selecting the largest value from the set. Thus, we add a new edge to the graph, e_{inter} and annotate it with a single capability and corresponding clearance value, $e_{inter}(c) = cv_{inter}$. The algorithm repeats for each $c \in C$ and terminates when all adjacent clusters have been considered. This ensures we identify all possible entrances for each available capability.

In Figure 2(b) we present three entrances identified by scanning the border between clusters $C1$ and $C3$. Entrances *E1* and *E2*, each of which span only part of the border area, are discovered using the $\{Ground\}$ and $\{Trees\}$ capabilities respectively. *E3* meanwhile, which spans the whole border area, is discovered using the $\{Ground \vee Trees\}$ capability. The connected tiles represent the locations of the subsequent transition points; the final result is shown in Figure 2(c). Note that *E1* and *E3* are incident on the same pair of nodes in the abstract graph. This is due to our strategy of actively attempting to re-use any existing nodes from the abstract graph.

The final step in the decomposition involves attempting to add to the abstract graph a set of *intra-edges* for each pair of abstract nodes inside a cluster. We achieve this by running multiple AA* searches $\forall(c, s) : c \in C, s \in S$. Once a path is found we annotate the new edge, e_{intra}, with the capability and clearance parameters used by AA* and set its weight equal to the cost of the path. The algorithm terminates when all clusters have been considered.

We thus construct an abstract *multi-graph* in which each edge e is annotated with a single capability c_e and associated clearance value cv_e. Each $e \in E_{abs}$ is traversable by an agent a iff:

$$e(c_a) = cv_e \geq s_a : c_e \subseteq c_a \in C, s_a \in S$$

Where c_a represents the capability of the agent and s_a its size. We term the resultant abstraction $initial$ and give the following lemmas to characterise its space complexity:

Lemma 3. *Let V_{abs} represent the set of nodes in an abstract graph of a gridmap which is perfectly divisible into $c \times c$ clusters, each of size $n \times n$. Then, in the worst case, the total number of nodes is given by:*

$$|V_{abs}| = 4(2n-1) + (4c-4)(3n-2) + (c-1)^2(4n-4)$$

Proof. Each transition point results in two nodes in the abstract graph. In the worst case the number of terrains $r \geq n$. If there are no hard obstacles and every pair of nodes along the adjacent border between two clusters has different terrain type then there will be a maximal number of transition points. In this scenario, clusters in the middle of the map, of which there are $(c-1)^2$, have 4 neighbours and each one contains $4n-4$ nodes. Clusters on the perimeter of the map (excluding corners), of which there are $4c-4$, have 3 neighbours and $3n-2$ nodes. Corner clusters, of which there are 4, have 2 neighbours and each contains $2n-1$ nodes. □

Lemma 4. *Let $E_{abs}(L) \subset E_{abs}$ represent the set of intra-edges for a cluster L that contains x abstract nodes. Further, let r be the total number of terrains found in the map and k the number of distinct terrain types found inside L. Then, the number of intra-edges required to connect all nodes in L is, in the worst case:*

$$|E_{abs}(L)| = |S| \times 2^{k-1} \times \frac{x(x-1)}{2}$$

Proof. For each pair of abstract nodes in a cluster and each size/capability combination, we compute at most one path of optimal length. From lemma 1 we know each node is

traversable at most by 2^{r-1} capabilities thus there must be at most $|S| \times 2^{r-1}$ ways of covering 2 nodes. However, the number of terrains inside a cluster is governed by its size; only $k \leq r$ terrains may be found. From this, it follows that the upper-bound on the size of the set of edges covering each pair of nodes is in fact $|S| \times 2^{k-1}$. In the worst case there will be a maximal number of edges between each pair of nodes and there are $\frac{x(x-1)}{2}$ such pairs in total per cluster. □

Lemma 5. *Let $E_{inter} \subset E_{abs}$ represent the set of inter-edges in an abstract graph of a grid map. In the worst case, the map is perfectly divisible into $c \times c$ clusters, each of size $n \times n$ and the number of inter-edges is given by*

$$|E_{inter}| = (2c^2 - 2c) \times \frac{n(n-1)}{2}$$

Proof. We know from the proof of lemma 3 that in the worst case each tile along the border between two adjacent clusters is represented by a node in the abstract graph. If we count the number of adjacencies, avoiding duplication, we find there are $2c^2 - 2c$ in total.

Each transition results in an inter-edge and there are n single-terrain transitions with clearance 1 per adjacency and some number of inter-edges to represent multi-terrain transitions with larger clearances. By observation we can see that that each adjacency will produce [n single-terrain transitions]...[1 n-terrain transition]. This recurrence relation holds for the general sequence counting formula $\frac{n(n-1)}{2}$ □

The above results are interesting for several reasons. Firstly, lemma 3 shows that the number of nodes in the graph is a function of cluster-size. This suggests that by varying the dimensions of clusters we can trade a little performance (the time it takes to traverse a cluster) for memory (less abstraction overhead). The results in lemma 4 and 5 seem to support this hypothesis. We see that the number of edges between nodes in the graph is mostly dependent on the complexity of the clusters in which they reside rather than exponential in the number of capabilities. This is exciting because it means that, despite having an exponential abstract edge growth function, we can directly control the size of the exponent! The cluster-based decomposition technique allows us to include as much or as little complexity in each cluster as we require.

Optimising Abstract Graph Size

As we have observed in lemmas 4 and 5 the initial abstraction algorithm attempts to represent every optimal path between clusters and inside clusters. However, most maps have far simpler topographies than the worst-case; in our experimental scenarios we often observed the same path returned for different pairs of (c, s) parameters when discovering intra-edges. This presents us with an opportunity to compact the graph by removing unnecessary duplication from the abstract edge set.

Consider the initial abstraction in Figure 3(a) and contrast it with our desired result in Figure 3(b). $\{E3, E5\}$ represent the same path between nodes w and y but are annotated with different clearance values. The same is true for $\{E4, E6\}$ which both cover nodes u and y. In such cases we say that $E3$ and $E4$ are *strongly dominant*, which we denote $E3 \succ E5$ and $E4 \succ E6$. This is an irreflexive and asymmetrical relationship between edges which we formalise with the following theorem:

Theorem 6. *Let $\{e_a, e_b\} \in E_{abs}$ be two edges which connect the same pair of abstract nodes and are annotated with capabilities $c_a \subseteq c_b \in C$ such that:*

$$1 \geq e_a(c_b) \geq e_b(c_b) \wedge weight(e_a) = weight(e_b)$$

Then $e_a \succ e_b$ and we may remove e_b from E_{abs} without loss of generality or optimality.

Proof. Since $c_a \subseteq c_b$ it must be the case that any agent with the correct capability to traverse e_b must be likewise able to traverse e_a. Further, if $e_a(c_b) \geq e_b(c_b)$ holds, it must also be the case that any agent large enough to traverse e_b is also large enough to traverse e_a. These conditions are sufficient to preserve generality. Finally, since e_a is equal in weight to e_b we cannot lose optimality by removing removing e_b. □

We term the resultant graph in which all strongly dominant edges have been removed a *high-quality* abstraction.

Figure 3: *Strong edge dominance*

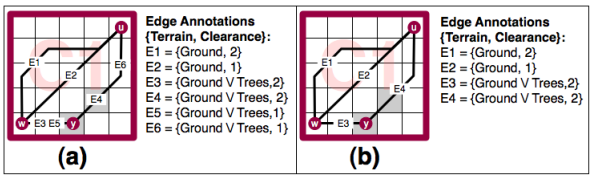

A further observation made during our analysis of this problem was that in many cases there exist multiple alternative routes to reach a goal location. The shortest paths tended to involve the traversal of optimal-length multi-terrain edges however, it was often possible to reach the same destination using slightly longer single-terrain edges. This suggests that the abstract graph can be further compacted without affecting the completeness of the representation.

A reasonable analogy to highlight our intuition here is to compare the way off-road vehicles opportunistically use roads where possible even if an off-road route of trail exists which has a smaller distance cost. We prefer roads because they connect most points of interest, are smoother to drive on and have other benefits such as less wear and tear and better fuel consumption.

Figure 4(a) and 4(b) show a typical high quality abstraction while in Figure 4(c) and 4(d) we highlight the desired result after further compacting the graph. In this example we can see that although edges $E1$ and $E2$ have different traversal requirements any agent of size $s \in S : S = \{1, 2\}$ capable of traversing $E2$ can also traverse $E1$ without loss of generality. In such cases we say $E1$ is *weakly dominant* and denote it as $E1 \succsim E2$. Notice also that $E3 \succsim E4$, $E6 \succsim E7$, $E10 \succsim E8$ and $E10 \succsim E9$.

As with theorem 6, this relationship is irreflexive and asymmetric. Unlike strong dominance however, only representational completeness (and not optimality) is retained. We formalise it as:

Figure 4: *High and low quality abstraction results*

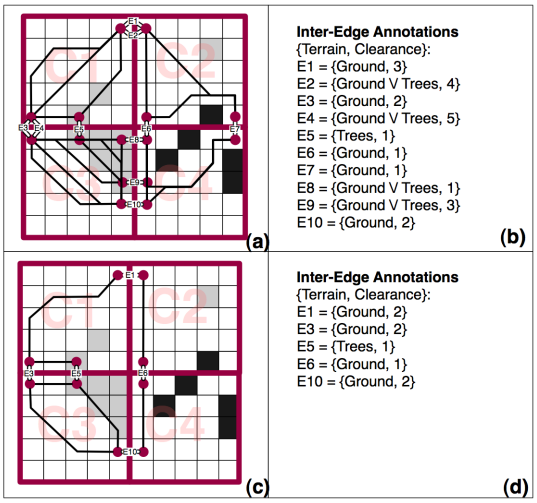

Theorem 7. *Let L_a and L_b be two adjacent clusters, and $\{w_a, x_b\}, \{y_a, z_b\} \in V_{abs}$ two pairs of abstract nodes, each pair connecting L_a and L_b. Denote the inter-edges associated with these node pairs as $\{e_{wx}, e_{yz}\} \in E_{abs}$ and suppose they are annotated with clearance values $e_{wx}(c_{wx}), e_{yz}(c_{yz}) : c_{wx} \subseteq c_{yz} \in C$. In this scenario, $e_{wx} \succsim e_{yz}$ iff the following conditions are met:*

1. *The capability dominance condition: $e_{wx}(c_{yz}) \geq e_{yz}(c_{yz})$.*
2. *The circuit condition: $\exists e_{wy}, e_{xz} \in E_{abs}$ which connect $\{w_a, y_a\}$ and $\{x_b, z_b\}$ such that $e_{wy}(c_{yz}) \geq e_{yz}(c_{yz})$ and $e_{xz}(c_{yz}) \geq e_{yz}(c_{yz})$.*

Then, any location which can be reached by traversing e_{yz} can also be reached via e_{wx}.

Proof. If a circuit exists between the set of edges $\{e_{wx}, e_{yz}, e_{wy}, e_{xz}\}$ in which every edge is traversable by c_{yz} with a clearance value at least equal to $e_{yz}(c_{yz})$, then it follows that any nodes in L_a or L_b which are reachable from y_a or z_b must be reachable from w_a or x_b. Thus, any destination an agent can reach via e_{yz} can also be reached via e_{wx}. □

Corollary 8. *If $e_{wx} \succsim e_{yz}$, then y_a and z_b and are also dominated and can be removed, unless required by another (non-dominated) inter-edge.*

Proof. If y_a and z_b are required by a non-dominated inter-edge we cannot remove them without violating the capability dominance condition which is required to retain representational completeness. If this is not the case however, we know by the circuit condition that any node reachable by an intra-edge via y_a or z_b is also reachable via the endpoints of e_{wx}. Thus, both nodes and any associated intra-edges dependent on them, can be safely removed. □

In many situations multi-terrain inter-edges tend to be associated with very large clearances; much larger than the size of our largest agent. This unnecessarily limits the applicability of the capability dominance condition from theorem 7. Leveraging the fact that $max(s) \in S$ is known, we can maximise the number of edges which are weakly dominated by applying the following truncation condition to E_{abs} before theorem 7:

$$e(c) > max(s) \Rightarrow e(c) = max(s) : s \in S, \forall e \in E_{abs}$$

Of course, opting for a low-quality abstraction in this way does affect the quality of computed solutions. In the worst case, a one-step transition of cost 1.0 in a high quality graph may be as long as $f(n) = 4n + f(n-2) : f(2) = 3, f(3) = 13$, where $n \geq 2$ is the length of a cluster in a low-quality approximation. This is a pathological case however; as we will show the differences in real-world scenarios are much smaller and still near-optimal. The choice of which quality abstraction technique to employ will depend on the requirements of the specific application; it is a classic tradeoff between run-time performance vs space.

Hierarchical Planning

Given a suitable graph abstraction, we can once more turn our attention back to agent planning. We use a similar process to that described in (Botea, Müller, and Schaeffer 2004) but in our case we substitute A* for AA*. We provide a brief overview of the process here; for a more detailed description, we direct the reader to the original work.

We begin by using the x, y coordinates of the start and goal nodes to identify the local cluster each is located in. Next, we insert a two temporary nodes into the abstract graph (which we remove when finished) to represent the start and goal. Connecting the nodes to the rest of the graph involves attempting to find an intra-edge from each node to every other abstract node in the cluster using AA*. This phase involves $i + j$ searches in total, corresponding to the number of combined abstract nodes in the start and goal clusters.

To compute a high-level plan we again use a variation on A* – this time to evaluate the annotations of abstract edges before adding a node to the open list. Once the search terminates we can take the result, and, if immediate execution is not necessary, we are finished. Otherwise, we refine the plan by performing a number of small searches in the original gridmap between each pair of nodes along the abstract optimal path.

We term the resultant algorithm Annotated Hierarchical A* (AHA* for short).

Experimental Setup

We evaluated the performance of AA* and AHA* on a set of 120 octile-based maps, ranging in size from 50x50 to 320x320, which we borrowed from a popular roleplaying game. The same maps were used by (Botea, Müller, and Schaeffer 2004) in their original study. In their default configuration the maps only featured one type of traversable terrain interspersed with hard obstacles. We therefore created five derivative sets (making for a total of 720 maps) where each traversable tile on every map had one of $\{10\%, 20\%, 30\%, 40\%, 50\%\}$ probability of being converted into a second type of traversable terrain (a soft obsta-

cle). This allowed us to evaluate the algorithms in environments featuring a range of soft and hard obstacles.

For each map we generated 100 experiments by randomly creating valid problems between an arbitrarily chosen pairs of locations and some random capability. We used two agent sizes in each experiment: small (occupying one tile) and large (occupying four tiles) resulting in 144000 problem instances (720x200) overall. All experiments were conducted on a 2.4GHz Intel Core 2 Duo processor with 2GB RAM running OSX 10.5.2. To implement both planners we used the University of Alberta's freely available pathfinding library, HOG (`www.cs.ualberta.ca/~nathanst/hog.html`).

Results

In Figure 5 we present the size of the abstract graphs relative to the size of the original graphs which featured an average 4469 nodes and 16420 edges. We look at the effect of increasing the amount of soft obstacles (SO) from 0% (the original test maps with only one traversable terrain) to 50%. We also contrast high and low quality abstractions (denoted HQ and LQ) on a range of cluster sizes $\{10, 15, 20\}$ (denoted CS10, CS15 and CS20).

Figure 5: *Size of abstract graph with respect to original graph.*

		0% SO	10% SO	20% SO	30% SO	40% SO	50% SO
CS10 HQ	Nodes	9.0%	14.6%	16.6%	17.7%	18.3%	18.5%
	Edges	8.2%	32.6%	38.4%	37.8%	35.7%	35.0%
CS10 LQ	Nodes	5.3%	7.9%	10.3%	12.8%	15.0%	15.7%
	Edges	2.2%	6.7%	11.6%	17.0%	22.0%	23.6%
CS15 HQ	Nodes	5.6%	9.6%	11.0%	11.8%	12.2%	12.3%
	Edges	6.0%	28.0%	32.4%	32.1%	30.0%	29.4%
CS15 LQ	Nodes	2.9%	4.8%	6.4%	8.1%	9.7%	10.3%
	Edges	1.2%	4.6%	8.5%	12.5%	17.2%	18.8%
CS20 HQ	Nodes	4.0%	7.0%	8.1%	8.8%	9.1%	9.2%
	Edges	5.0%	25.0%	28.8%	28.3%	26.3%	26.0%
CS20 LQ	Nodes	2.0%	3.4%	4.6%	5.9%	7.2%	7.6%
	Edges	0.9%	3.6%	6.9%	10.1%	14.4%	15.8%

The first thing to notice is that in all cases the abstract graph is only a fraction the size of the original graph. As expected, larger clusters generate smaller graphs; the smallest abstractions are observed on the SO 0% problem set using CS20. In this case, using a HQ abstraction results in 4.0% the number of nodes found in the original graph and 5.0% edges. LQ abstractions fare even better featuring just 2.0% as many nodes and 0.9% edges.

The total space complexity associated with storing a graph is given by the total amount of space required to store both nodes and edges. If we assume each non-abstract node and edge require one byte of memory to store, then our smallest abstract graph, which contains 2 annotations per edge (capability and clearance, together requiring 1 additional byte), will have a space complexity 8.7% the size of the original graph using a HQ abstraction and just 1.8% using an LQ abstraction. Similarly, the largest HQ graph, which occurs for CS10 on SO 20%, has a space complexity 63.8% the size of the original. By comparison, LQ graphs are largest for CS10 on SO 50%; here 40.4% the size of the original gridmap. Moving from CS10 to CS20 reduces the worst-case space complexity of HQ graphs to 47.0% and 26.4% for LQ graphs.

Interestingly, if we use the number of nodes as an indicator for the number of inter-edges in a graph, we may deduce that most HQ graphs are predominately composed of intra-edges. The exact number depends on the density of soft obstacles in clusters; less dense clusters (as found on SO 20%) result in more intra-edges as more unique paths (of differing sizes and capabilities) are found between each pair of abstract nodes. This is consistent with lemma 4 and useful to understanding the worst-case behaviour of HQ abstractions.

The linear increase in the size of LQ graphs is the result of a greater number of single-terrain entrances found as the number of soft obstacles increases (an observation consistent with lemma 3). Increasing the density of soft obstacles in a cluster causes the circuit condition from theorem 7 to be less often satisfied and leads to the observed worst-case on SO 50%.

Next we consider the performance of AHA* with respect to path quality. We measure this as:

$$\%error = \frac{apl - opl}{opl} \times 100$$

where opl is the length of the optimal path as calculated by AA* and apl the length of the abstract path used by AHA*.

Figure 6: *AHA* performance (HQ vs LQ abstraction)*

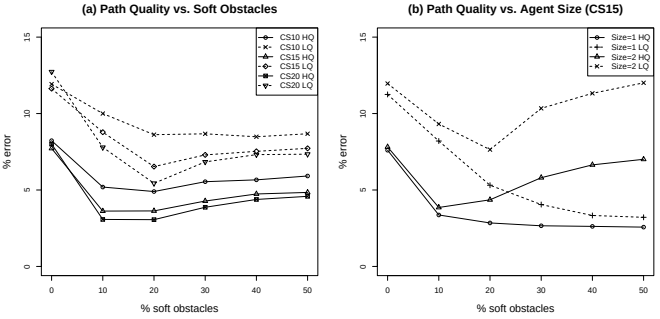

Figure 6(a) shows the average performance of AHA* with respect to cluster size and soft obstacles. Notice that HQ graphs yield a very low error; in most cases between 3-6%. Perhaps most encouraging however are the results for LQ abstractions, where in most cases AHA* performs within 6-10% of optimal. The highest observed error in both cases occurs on SO 0% and is due to our inter-edge placement strategy. In all situations the pair of nodes with maximal clearance in an entrance, which we choose as our transition point, tends to be towards the beginning of the entrance area which is not an optimal placement. On maps that produce low-complexity clusters of predominately one terrain this results in long entrances that are poorly represented by the single inter-edge. Increasing the amount of soft obstacles produces shorter entrances and generates more transition points leading to a significant reduction in error. It appears AHA* is so optimised for complex cases that it suffers some minor performance degradation on simpler problems.

Interestingly, the error associated with both HQ and LQ abstractions reaches a minimum on SO 20% before gradually increasing toward SO 50%. To better understand this

phenomenon we present in Figure 6(b) the performance of both small and large agents on HQ and LQ graphs using a fixed cluster-size of 15. Notice that the performance of small agents continues to improve beyond SO 20% while large agents begin to degrade. The observed rise in error stems from the decreasing size of entrances on the problem sets featuring denser clusters. As previously shown in Figure 5, maps with more soft obstacles result in a greater number of smaller entrances. This situation is beneficial for smaller agents (there are more transitions to choose from) but is disadvantageous for larger agents. As the average entrance size shrinks fewer inter-edges exist with clearance > 1 and the location of such edges along the border area between clusters may be quite varied; sometimes we find an entrance toward the beginning of the border area, other times in the middle and sometimes toward the end. Consequently, cluster traversal by large agents is often not in a straight line; the abstract paths produced frequently feature a zig-zagging effect that is responsible for the observed error and is most pronounced on SO 50%.

Figure 7: *AHA* total search effort (nodes expanded).*

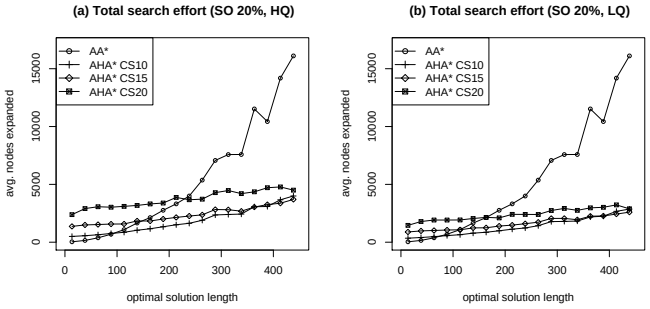

Finally, we turn our attention to Figure 7 where we evaluate AHA* using a search effort metric. Here we contrast the total number of nodes expanded by AHA* (during insertion, hierarchical search and refinement phases) with AA* on both HQ and LQ graphs. We focus on the SO 20% problem set in order to analyse the effect on search effort as path length increases but note that similar trends hold for the other problem sets.

Looking at Figure 7(a) we observe that agents using HQ graphs featuring large cluster-sizes are disadvantaged in this test. The insertion effort required to connect start and goal to each abstract node in their local clusters heavily dominates the total effort causing AHA* CS20 to trail AA* for problems up to length 250. We can see the gap between CS20 and the smaller cluster sizes decrease as problem size grows but our benchmark set of experiments are not hard enough for such coarse-grain map decompositions to be advantageous. By comparison, in Figure 7(b) we see that the difference is less pronounced using LQ graphs (there are less abstract nodes per cluster) however it appears CS10 or CS15 are more suitable choices for problems up to our maximum length, 450.

Conclusion

Heterogeneity in path planning is characteristic of many real-world problems but has received very little attention to date. In this paper we have addressed this issue by showing how clearance-based obstacle distances can be computed and leveraged to improve path planning for multi-size agents in heterogenous-terrain grid-world environments. Our approach reduces complex problems involving agents of different sizes and multi-terrain traversal capabilities to much simpler single-size, single-terrain search problems. Building on these new insights, we have introduced a new planner, Annotated Hierarchical A*, and have shown through comparative analysis that AHA* is able to find near-optimal solutions to problems in a wide range of environments yet still maintain exponentially lower search effort over standard A*. Our hierarchical abstraction technique is simple to apply but very effective; we have shown that in most cases the overhead for storing the abstract graph is a small fraction of that associated with non-abstract graphs.

Future work could involve looking at computing annotations to deal with elevation and other common terrain features. We are also interested in finding a better inter-edge placement approach and reducing the effort to insert the start and goal into the abstract graph. Finally, we believe AHA* could be usefully applied to solving heterogenous multi-agent problems.

Acknowledgements

NICTA is funded by the Australian Government as represented by the Department of Broadband, Communications and the Digital Economy and the Australian Research Council through the ICT Centre of Excellence program.

We would like to thank Philip Kilby and Eric McCreath for their help and insightful comments during the development of this work.

References

Botea, A.; Müller, M.; and Schaeffer, J. 2004. Near optimal hierarchical path-finding. *Journal of Game Development* 1(1):7–28.

Demyen, D., and Buro, M. 2006. Efficient triangulation-based pathfinding. In *AAAI*, 942–947.

Geraerts, R., and Overmars, M. 2007. The corridor map method: a general framework for real-time high-quality path planning. *Computer Animation and Virtual Worlds* 107–119.

Hart, P. E.; Nilsson, N. J.; and Raphael, B. 1968. A formal basis for the heuristic determination of minimum cost paths. *IEEE Transactions on Systems Science and Cybernetics* (4):100–107.

Latombe, J. 1991. *Robot Motion Planning*. Kulwer Academic Publishers.

Sturtevant, N. R., and Buro, M. 2005. Partial pathfinding using map abstraction and refinement. In *AAAI*, 1392–1397.